

Local Disturbances Preceding a Running Crack Front in a Viscoelastic Solid

AKIRA KOBAYASHI, MASAYUKI MUNEMURA, and NOBUO OHTANI,
*Institute of Space and Aeronautical Science, University of Tokyo, Komaba,
Meguro-ku, Tokyo, 153, Japan*

Synopsis

The local disturbances ahead of a running crack front in a viscoelastic solid were measured through noncontact electro-optical tools. It was observed that the very high local strain rate up to 200/sec exists even in the present quasistatic loading case. It may be concluded that the running crack propagation velocities, not the conventional average strain rates ranging from about 10^{-4} /sec to 10^{-2} /sec, govern the local disturbances, as the crack propagation velocities always exceed 200 m/sec for both average strain rates, while the local strain rates observed do not show much differences between both average strain rate cases.

INTRODUCTION

It is necessary to study about local disturbances or local deformations preceding a running crack front in order to investigate the dynamic crack propagation phenomenon. In the present report, the very local disturbances just preceding a running crack front during dynamic crack propagation in a viscoelastic solid are measured through noncontact electro-optical tools, from which the local strain rates are calculated to study correlations with running crack front locations.

EXPERIMENTAL

The local strain rates $\dot{\epsilon}$ are obtained in a noncontact electro-optical way, in which the preceding local disturbances are measured for a 5-mm gage length along the expected crack propagation passage on a specimen surface.

Noncontact Electro-Optical Measurement Instrument

An electro-optical extensometer Zimmer model 200X made by Bundesrepublik Deutschland (Fig. 1) was used to measure the relative instantaneous displacement between a 5-mm gage length at the middle of specimen width during the dynamic crack propagation. Principle of operation is described in the Appendix.

Specimen

Polymethyl methacrylate (PMMA) specimen (Fig. 2) was made of Sumipex virgin sheet, a product of Sumitomo Chemical Company, Japan. Velocity gages, consisting of du Pont conductive silver coating material No. 4817, were fixed on

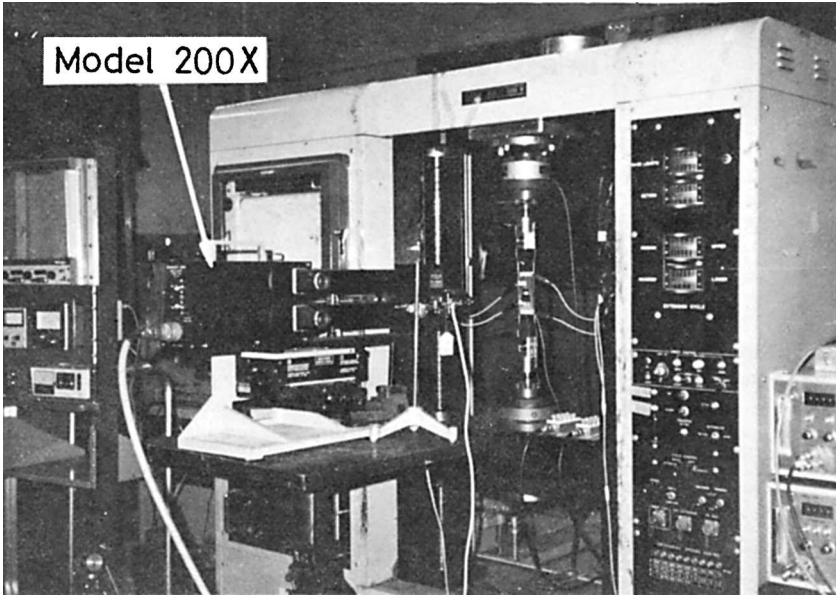


Fig. 1. Electro-optical extensometer Zimmer model 200X and the testing apparatus.

the specimen surface to measure the dynamic crack propagation velocity as shown in Figure 3.¹

Loading Apparatus

Toyo-Baldwin's Instron-type tensile tester, UTM-1, was employed both at 5 mm/min crosshead speed equivalent of $\dot{\epsilon}_A = 3.03 \times 10^{-4}/\text{sec}$ and at 500 mm/min equivalent of $\dot{\epsilon}_A = 3.03 \times 10^{-2}/\text{sec}$ to give tension loading to a specimen to initiate the mode I crack propagation, where the average strain rate $\dot{\epsilon}_A = \text{crosshead speed}/\text{gage length}$ (5 mm).

Measuring Block Diagram

A measuring block diagram is shown in Figure 4. A transient converter TCED-1000 of Riken Denshi Co. Japan was used as a digital memory.

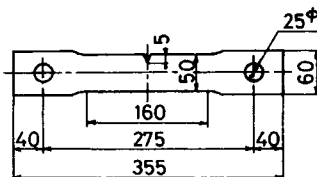


Fig. 2. Specimen.

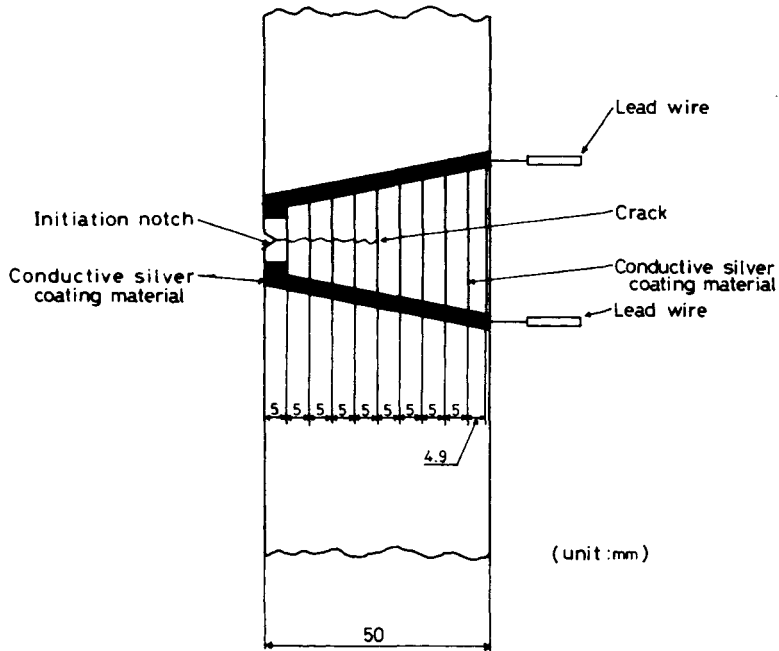


Fig. 3. Velocity gage arrangement.

EXPERIMENTAL RESULTS AND DISCUSSIONS

Crack Propagation Velocity \dot{C} vs. Nondimensional Crack Front Location

As shown in Figure 5, the crack propagation velocity \dot{C} vs. nondimensional crack front location C/W relation represents a tendency similar to those obtained previously.¹ It is observed that \dot{C} shows as high as 200–400 m/sec even for the quasistatic loading of $\dot{\epsilon}_A \approx 10^{-2}/\text{sec}$ to $10^{-4}/\text{sec}$. In Figure 5, C is a running crack front location and W is a specimen width (= 50 mm).

Relative Displacement δ vs. Distance to a Running Crack Front Y

The relative displacement δ observed between the 5-mm gage length, measured at $C/W = 0.5$, i.e., $Y = 0$, where Y is the distance between the running crack front and the noncontact measuring position ($C/W = 0.5$), by the electro-optical extensometer, increases as the running crack front approaches the noncontact

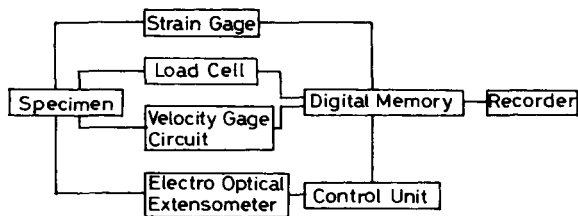


Fig. 4. Measuring block diagram.

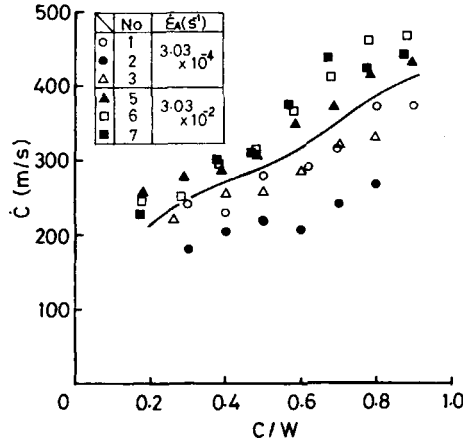


Fig. 5. Crack propagation velocity \dot{C} vs. nondimensional crack front location C/W .

measuring position, and shows a maximum value of about 0.08 mm at $Y = 0$ as shown in Figure 6.

Local Strain Rate $\dot{\epsilon}$ vs. Nondimensional Crack Front Location C/W

The local strain rate $\dot{\epsilon}$ is determined from δ data combined with the time scale, i.e., $\dot{\epsilon} = (d\delta/dt)/5 \text{ mm}$, and thus obtained local strain rate $\dot{\epsilon}$ is shown as a function of C/W as seen in Figure 7. It is noteworthy that there exist almost no differences between $\dot{\epsilon}_A = 3.03 \times 10^{-4}/\text{sec}$ case and $\dot{\epsilon}_A = 3.03 \times 10^{-2}/\text{sec}$ case.

Local Strain Rate $\dot{\epsilon}$ vs. Distance to a Running Crack Front Y

As shown in Figure 8, the local strain rate $\dot{\epsilon}$, obtained at the noncontact measuring location, $C/W = 0.5$, increases as the crack front approaches, and $\dot{\epsilon}$ becomes almost 200/sec when $Y = 0$, irrespective of average strain rate $\dot{\epsilon}_A$.

Considering the scatters in Figures 7 and 8, the difference due to $\dot{\epsilon}_A$ is scarcely observed for the present experimental cases of $\dot{\epsilon}_A = 3.03 \times 10^{-4}/\text{sec}$ and $3.03 \times$

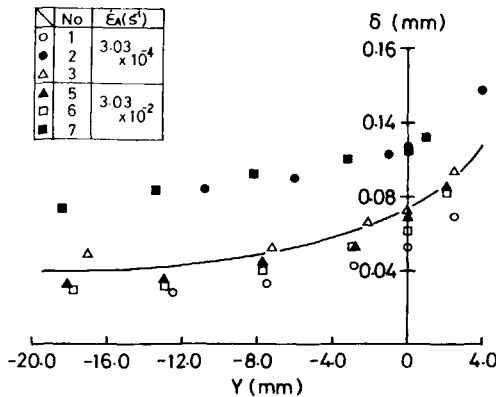


Fig. 6. Relative displacement δ vs. distance to a running crack front Y .

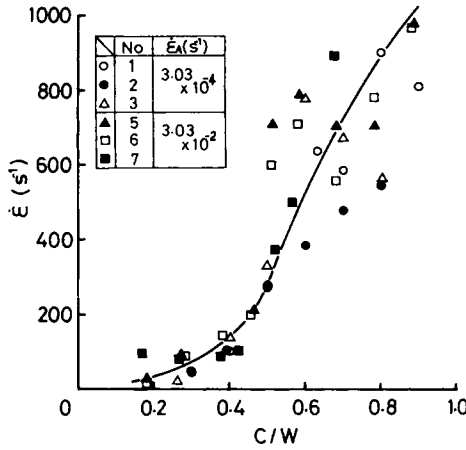


Fig. 7. Local strain rate $\dot{\epsilon}$ vs. nondimensional crack front location C/W .

$10^{-2}/\text{sec}$. $\dot{\epsilon}/\dot{\epsilon}_A = 7,000 \sim 700,000$ tells that the very large local strain rate is produced ahead of a running crack front. Judging from the fact that the crack propagation velocity exceeds 200 m/sec for any average strain rate, the large local strain rates seem to be dependent upon the crack propagation velocity rather than the average strain rate $\dot{\epsilon}_A$.

CONCLUSIONS

Local disturbances preceding a running crack front in a viscoelastic solid were measured by a noncontact electro-optical extensometer, finding very high local strain rate up to 200/sec even for the quasistatic loading case of 5-mm/min crosshead speed. It may be concluded that the very running crack propagation

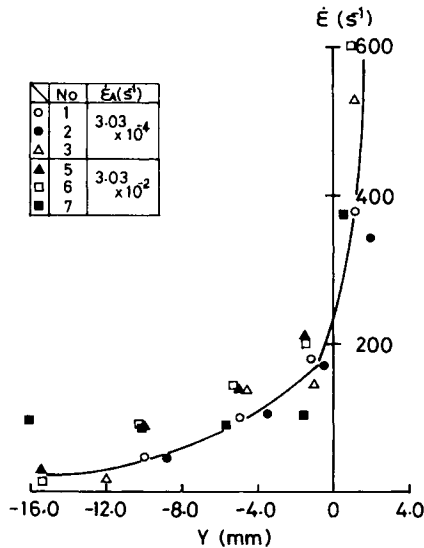


Fig. 8. Local strain rate $\dot{\epsilon}$ vs. distance to a running crack front Y .

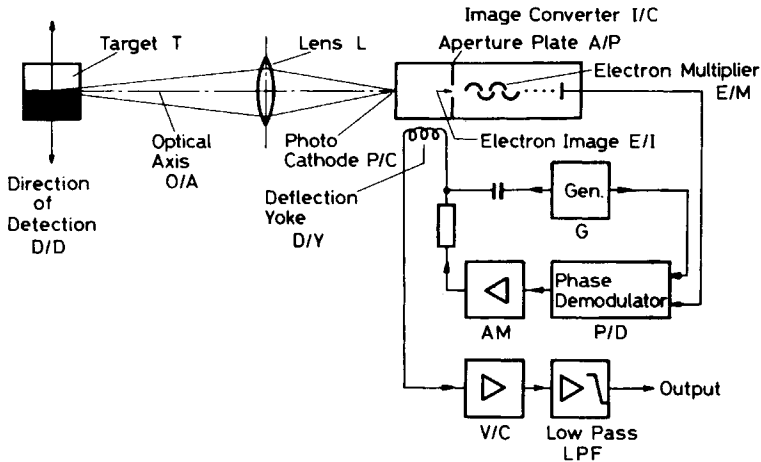


Fig. 9. Block diagram of principle of operation for model 200X.

velocity, not the average strain rate, governs the local strain rate produced in disturbances preceding a running crack front.

The authors thank Haruo Kobayashi, Kenji Kodama, and Yoshinari Fujii for their assistance.

APPENDIX

The electro-optical extensometer Zimmer model 200X consists of two identical and independent displacement transducer systems (Fig. 9).

Each displacement transducer system works as follows: A lens (L) projects an image on the photo cathode (P/C) of the image converter (I/C) of the model 200X. The optical image is converted into an electron image (E/I) by the P/C. It is then projected on an aperture plate (A/P). A deflection yoke (D/Y) between P/C and aperture plate (A/P) permits fast deflection of the E/I without inertia.

The D/Y is driven by a generator (G). This causes the output of the electron multiplier (E/M) to generate pulses. These pulses are in phase with the generator signal if the target center line is located on the optical axis (O/A). A phase demodulator (P/D) converts the phase relationship between both signals into an analog voltage, which is zero at zero phase shift.

An amplifier (AM) connected to the output of the phase demodulator applies the control signal to the D/Y. This results in a closed loop scanning system. The electron image is always kept in position even if the target (T) moves in the direction of detection (D/D).

The correcting current in the D/Y keeps the E/I in a fixed position and is proportional to the target deflection. A current to voltage converter (V/C) with a low pass filter (LPF) in the output generates the signal proportional to displacement.

Reference

1. A. Kobayashi, N. Ohtani, and T. Sato, *J. Appl. Polym. Sci.*, **18**, 1625 (1974).

Received August 5, 1980

Accepted December 18, 1980